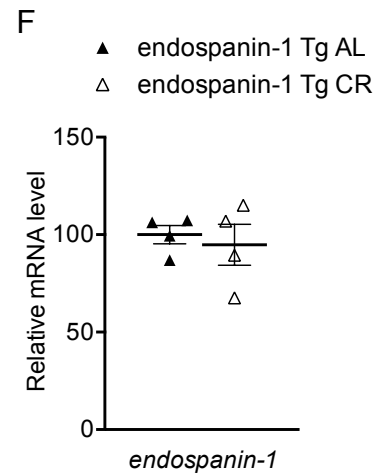
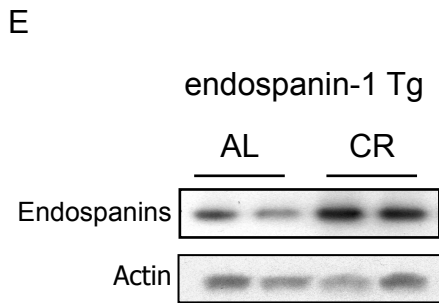
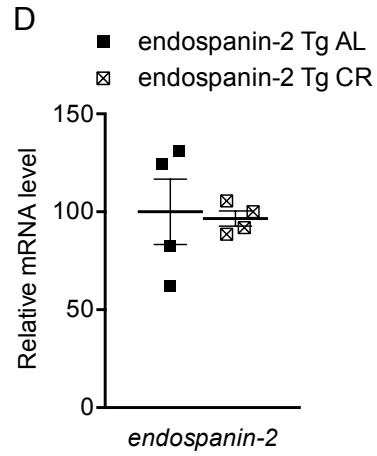
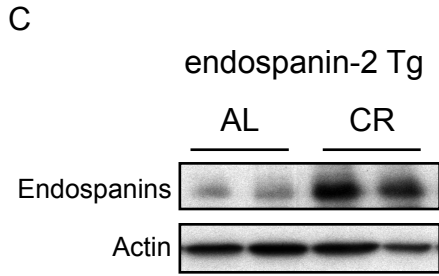
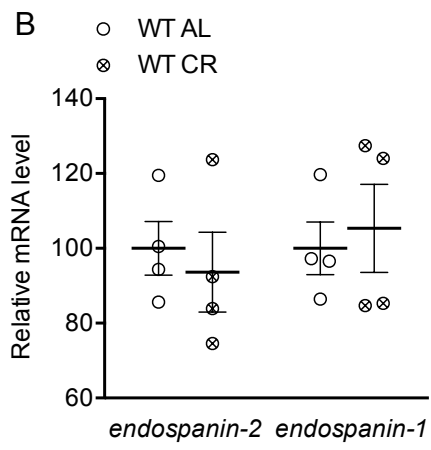
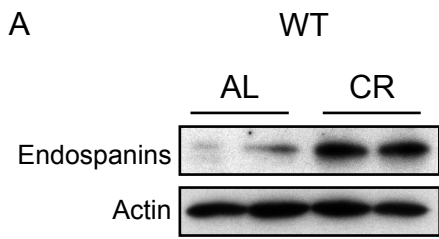
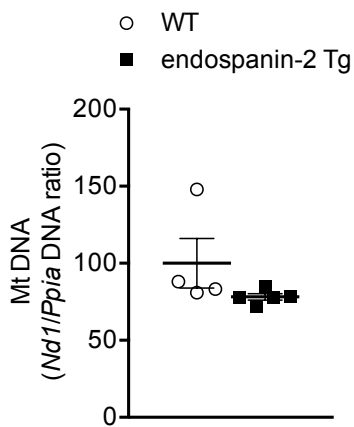
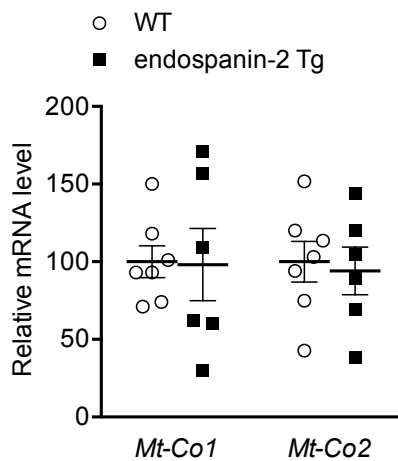
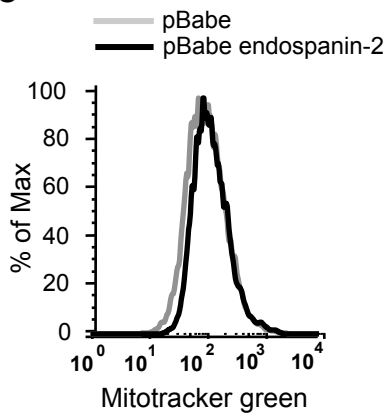
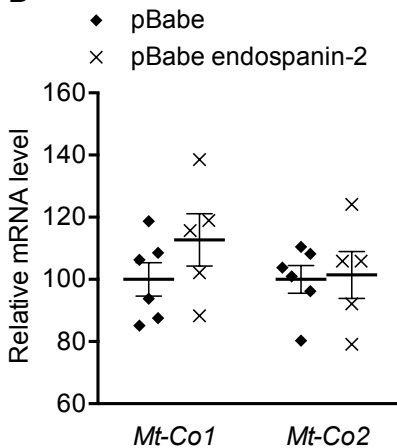
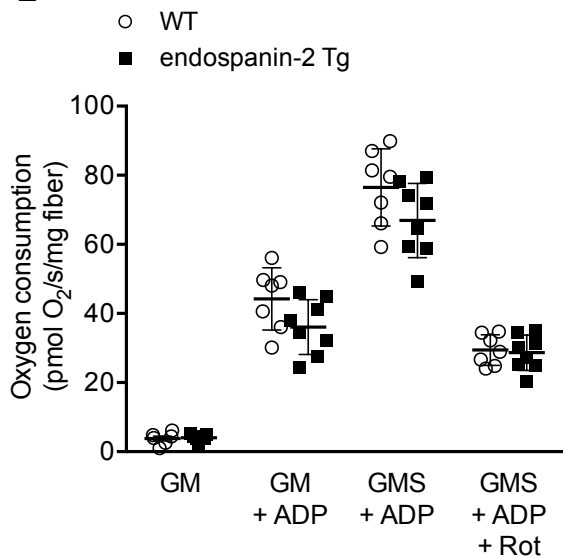
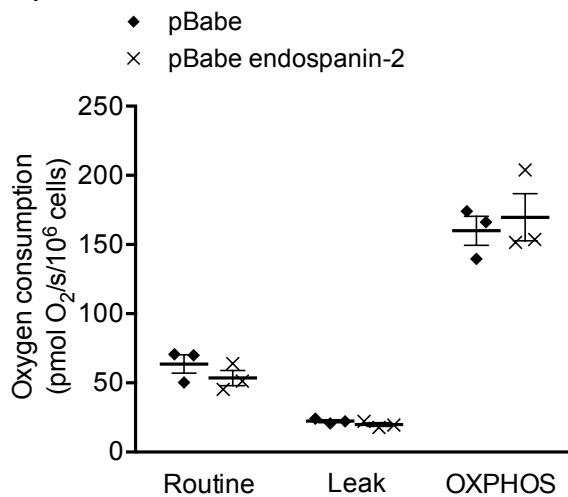


## **Supplemental data includes:**

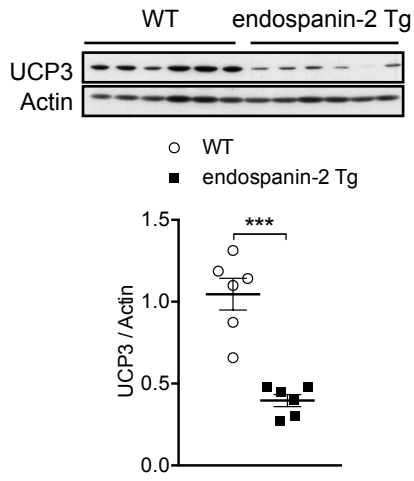
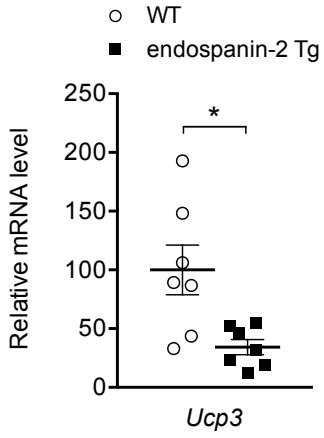
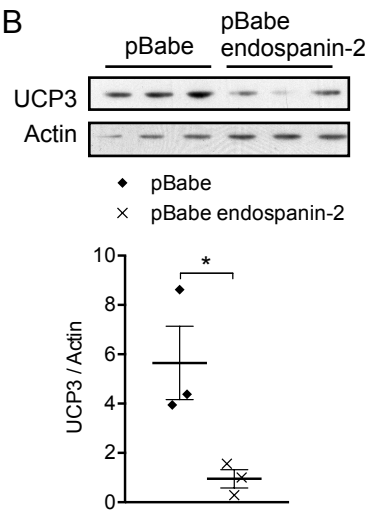
- **Supplementary figures and legends S1-S8**
- **Table S1**
- **Extended experimental procedures**



**Figure S1:** Western blot analysis of endogenous endospanins protein levels in quadriceps muscle **(A)** from WT mice, **(C)** from endospanin-2 Tg mice and **(E)** from endospanin-1 Tg mice fed *ad libitum* (AL) or subjected to 4 weeks of CR ( $n = 2$ ) using antibodies against the C-ter of both endospanins. RT-qPCR analysis of **(B)** endogenous *endospanin-1* and *endospanin-2* mRNA levels in skeletal muscle from WT mice, **(D)** *Endospanin-2 transgene* mRNA levels and **(F)** *Endospanin-1 transgene* mRNA levels in quadriceps muscle from endospanin-2 Tg mice and endospanin-1 Tg mice, respectively, fed *ad libitum* or subjected to 4 weeks of CR ( $n = 4$ ).

**A****B****C****D****E****F**

**Figure S2:** (A) Mitochondrial DNA (mtDNA) content (normalized to nuclear *Ppia* DNA) in quadriceps muscles endospanin-2 Tg mice and their WT littermates (n = 6 per condition). (B) RT-qPCR analysis of the two complex IV subunits (*Mt-Co1* and *Mt-Co2*) of the mitochondrial respiratory chain mRNA levels normalized to *Ppia* mRNA level in quadriceps muscles from endospanin-2 Tg mice and their WT littermates (n = 6 per condition). (C) Representative histograms of flow cytometry staining using mitotracker green (MT) illustrating mitochondria content in differentiated endospanin-2 or control (pBabe) retrovirus-infected C2C12 cells (n = 6 per condition). (D) RT-qPCR analysis of *Mt-Co1* and *Mt-Co2* mRNA levels normalized to *Ppia* mRNA level in differentiated endospanin-2 or control pbabe C2C12 cells (n = 5 per condition). (E) Mitochondrial respiration in permeabilized EDL fibers: O<sub>2</sub> flux measured in isolated EDL fibers and expressed per mg of wet weight. Mitochondrial substrates were sequentially added: 10 mM glutamate + 2 mM malate in absence (GM) or in presence of 2 mM adenosine di-phosphate (GM+ADP) (State 3), +/- 10 mM succinate (GMS+ ADP) and 1 μM rotenone (GMS+ADP+Rot). All experiments were performed on fibers isolated from endospanin-2 and wild-type muscle (n = 7 per genotype). (F) Oxygen consumption in endospanin-2 and control pBabe cells (n = 5 per condition). 'Routine' represents basal respiration (without addition of exogenous substrate), leak (4O) is measured in presence of oligomycin and represents uncoupled respiration (*i.e.* proton leakage), OXPHOS (3U) is measured in presence of FCCP and represents the maximal respiratory capacity. Results are expressed as means ± sem

**A****B**

**Figure S3:** (A) RT-qPCR analysis of *Ucp3* mRNA levels normalized to *Ppia* mRNA level and western blot analysis of UCP3 protein level in quadriceps muscle from endospanin-2 Tg mice and their wild-type littermates (n = 6 per genotype) and in (B) differentiated C2C12 cells infected with endospanin-2 or control (pBabe) retrovirus (n = 3 per condition). Results are expressed as means  $\pm$  sem; \* p < 0.05, \*\* p < 0.01, \*\*\* p < 0.001 by unpaired t-test.

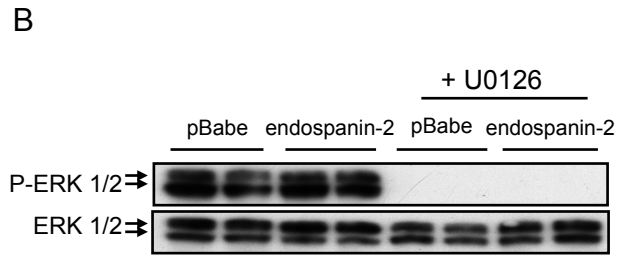
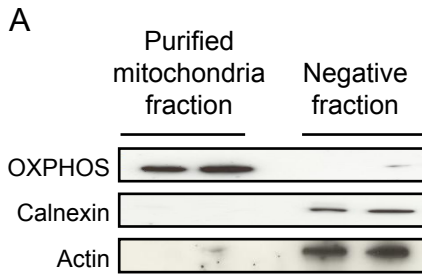
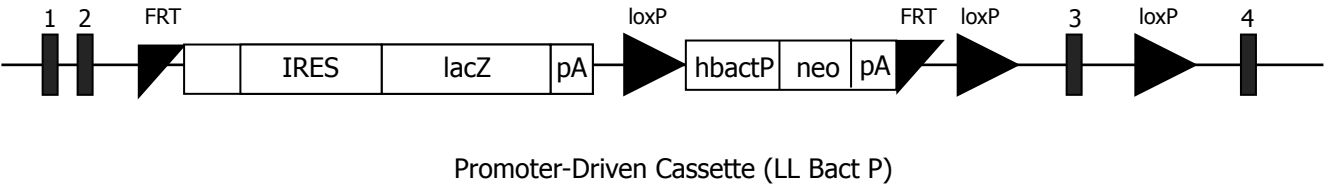


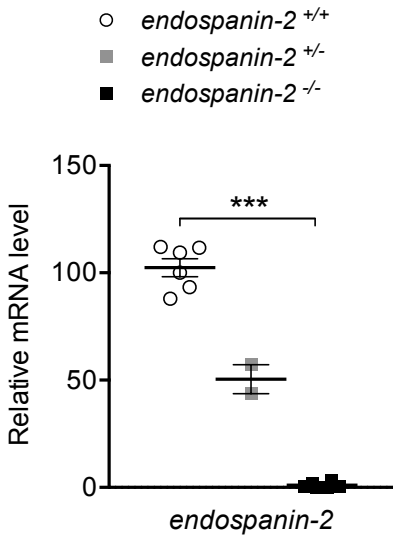


**Figure S4:** (A) Control of mitochondria fraction purity isolated using superparamagnetic microbeads conjugated to anti-TOM22 antibody (Myltenyi Biotech) following manufacturer's directions by western blot analysis using OXPHOS, calnexin and actin antibodies. (B) Control of U0126 efficiency by western blot analysis of Erk 1/2 phosphorylation and total Erk1/2 protein levels on endospanin-2 and control (pBabe) C2C12 cells incubated or not with U0126.

A



B



C

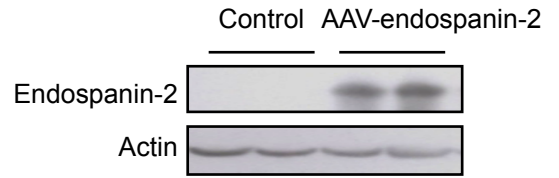


**Figure S5:** (A) *Leprotl1*<sup>tm1a(EUCOMM)hmg</sup> ES cells (EUCOMM) construct used to generate *endospanin-2*<sup>-/-</sup> mice (see methods). (B) RT-qPCR analysis of *endospanin-2* mRNA levels normalized to *Ppia* mRNA level in quadriceps from *endospanin-2*<sup>+/-</sup> heterozygous, *endospanin-2*<sup>-/-</sup> homozygous mice and their wild-type littermates (n = 2/6/genotype). (C) Western blot analysis of endospanin-2 protein levels in gastrocnemius muscle from mice intra-muscularly injected with a *endospanin-2* expressing AAV vector and a control AAV vector (n = 2 per group). Results are expressed as means ± sem; \*\* p < 0.01 and \*\*\* p < 0.001 by unpaired t-test.



**Figure S6:** (A) Densitometric analysis of western blot of Ulk1, Atg5, Beclin and LC3-I and LC3-II proteins levels in EDL muscle from endospanin-2 Tg mice compared to WT littermates (n=5-6/genotype) (B) Western blot analysis of soleus muscle Ulk1 in endospanin-2 Tg mice compared to wild-type littermates (n = 4-5 per genotype) (C) Representative images of immunofluorescence staining depicting single staining of lysosome (grey), LC3-II (red), endospanin-2 (green) and DAPI (blue) in endospanin-2 overexpressing C2C12 chloroquine(50  $\mu$ M) treated compared to control cells (n = 3 per condition).

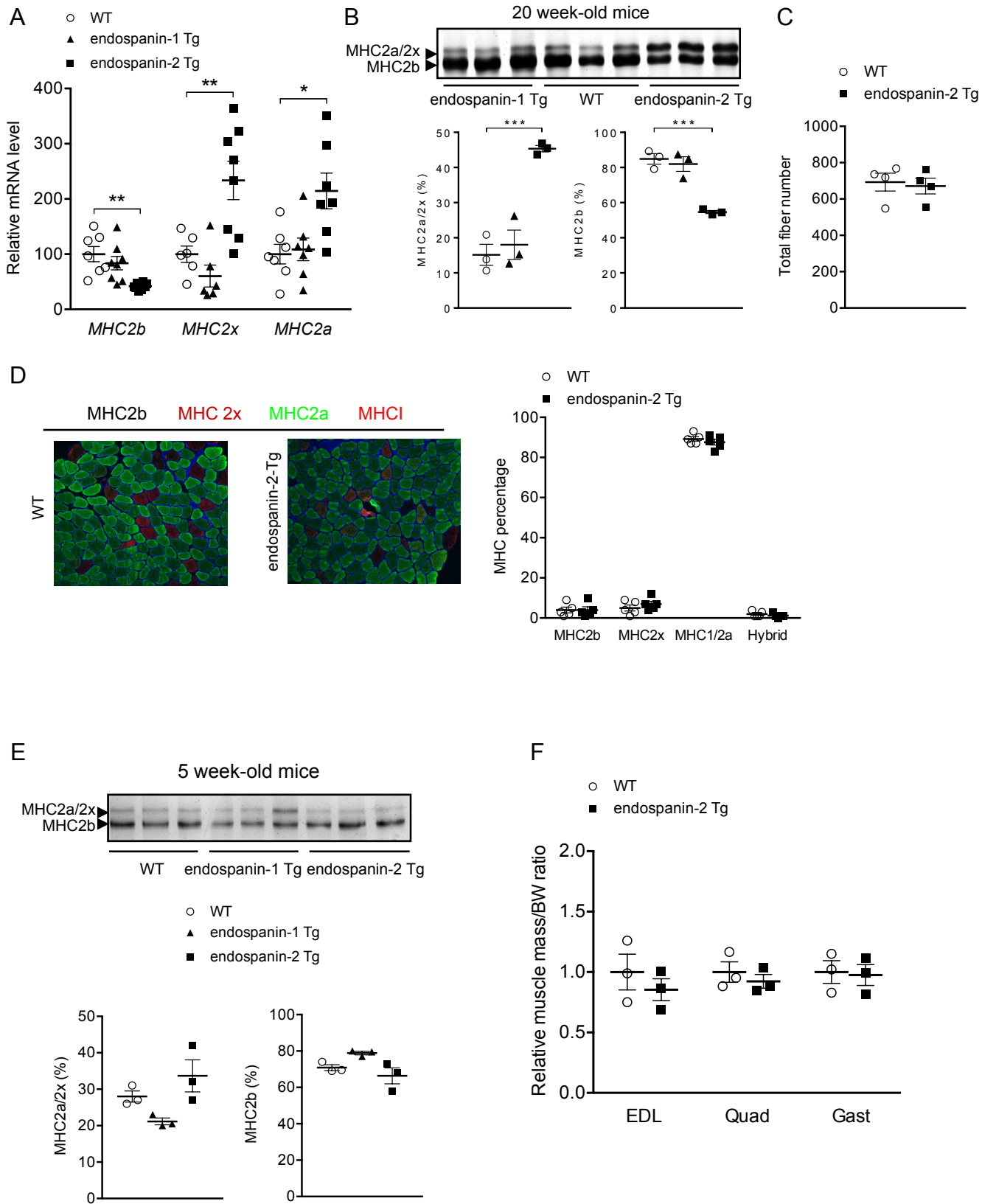


**Figure S7:** (A) RT-qPCR analysis of MHC2b, 2x and 2a mRNA levels, normalized to *Ppia* mRNA level, in EDL muscles from 20-week-old endospanin-1 Tg and endospanin-2 Tg mice compared to their wild-type littermates (n = 5 per group). (B) Electrophoretic determination of MHC isoforms in EDL muscles from 20-week-old endospanin-1 Tg and endospanin-2 Tg mice and their wild-type littermates (n = 3 per genotype). MHC2b and MHC2x isoforms were identified in increasing order of their electrophoretic mobility. (C) Evaluation of total fiber number of EDL from endospanin-2 Tg mice and their WT littermates (n = 5-6 per genotype). (D) Representative images of immunofluorescence staining of Myosin Heavy Chain (MHC) and percentage fiber typing of MHC1/2a (green), MHC2x (red), MHC2b (black) and hybrid (2a and 2x) on soleus sections from endospanin-2 Tg mice compared to their WT littermates (n = 5-6 per genotype). Individual muscle fibers were visualized in blue (laminin staining). (E) Electrophoretic determination of MHC isoforms in EDL muscles from 5-week-old endospanin-1 Tg and endospanin-2 Tg mice and their wild-type littermates (n = 3 per genotype). (F) Muscle mass relative to body weight of 5-week-old endospanin-2 Tg mice and their wild-type littermates (n = 3 per genotype).

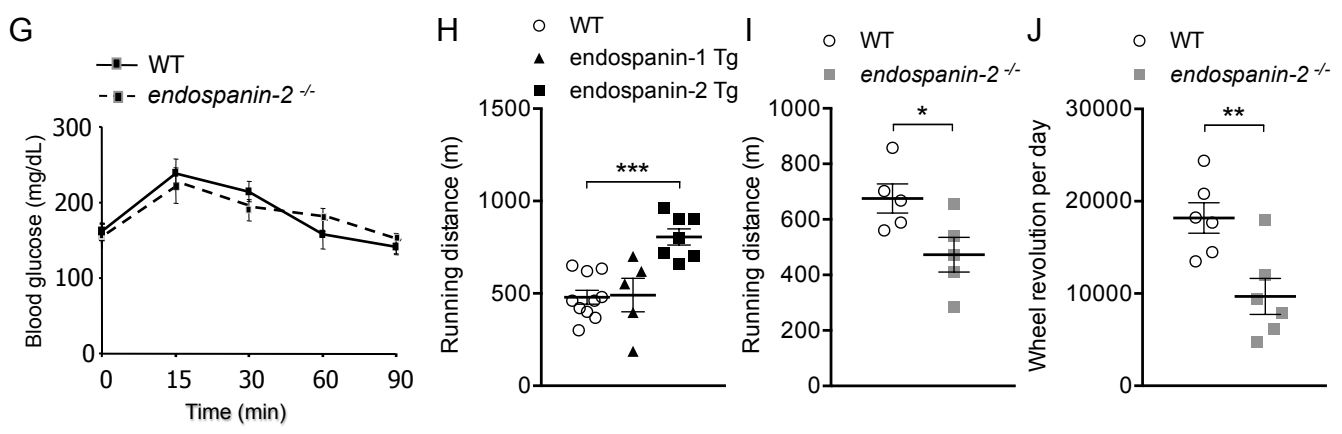
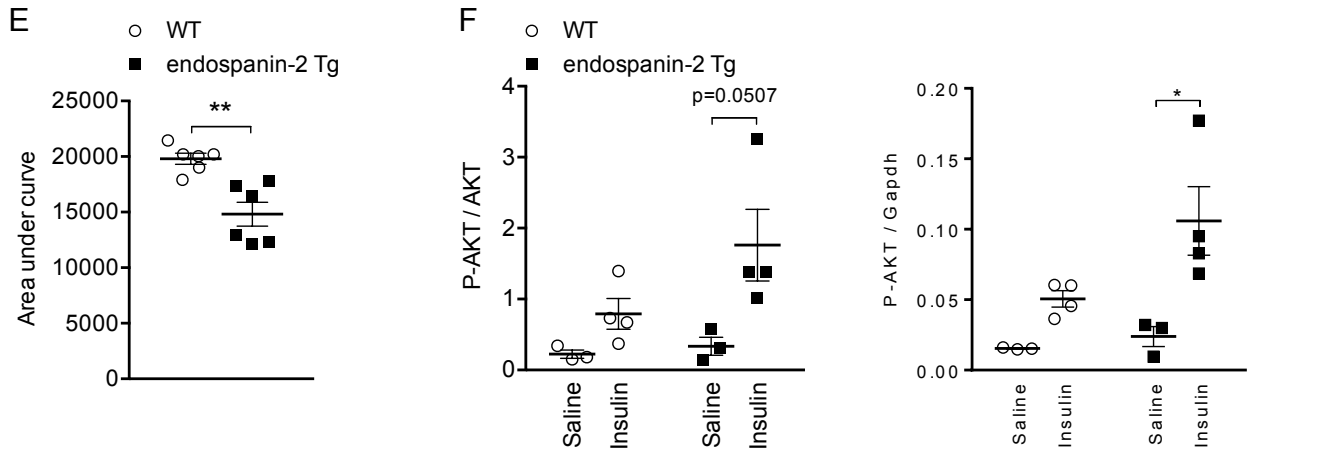
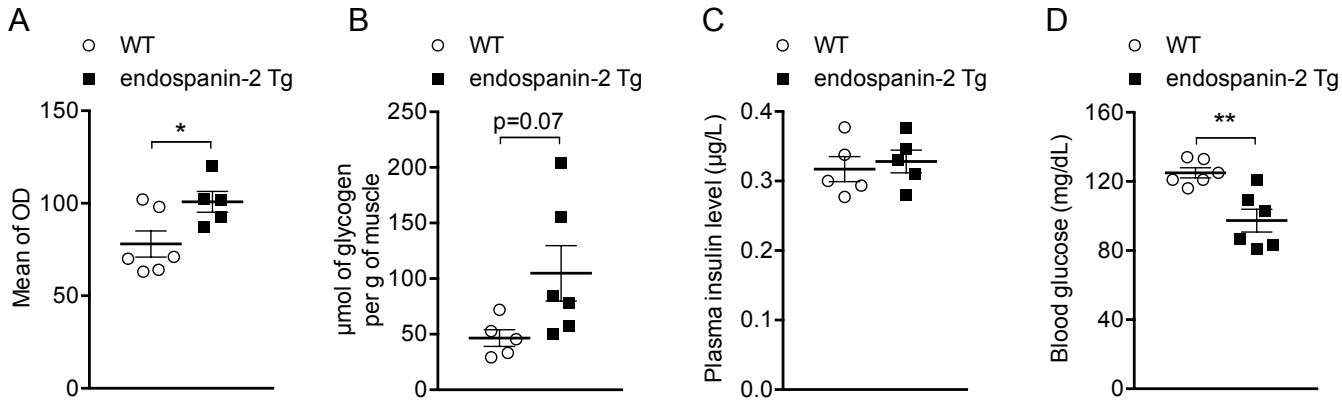




**Figure S8** (A) PAS staining optical density quantification (B) Evaluation of glycogen content by biochemical assay in EDL from endospanin-2 Tg mice compared to their wild-type littermates (n = 5-6 per group). (C) Fasting plasma insulin levels in endospanin-2 Tg mice and their wild-type littermates (n=5 per genotype) (D) Fasting plasma glucose level of endospanin-2 Tg mice and their wild-type littermates (n=6 per genotype). (E) Area under the curve of the IPGTT endospanin-2 Tg mice compared to their WT littermates (n=6-7 per genotype) (F) Densitometric analysis of western blot of P-AKT and AKT in quadriceps muscle from endospanin-2 Tg mice compared to WT littermates in basal and insulin-stimulated conditions (G) Intraperitoneal glucose tolerance test (1g/kg body weight) of *endospanin-2<sup>-/-</sup>* mice and their WT littermates (n= 6 per genotype) (H) Running distance in endurance exercise of endospanin-1 Tg and endospanin-2 Tg mice compared to their WT littermates (n = 5-10 per genotype). (I) Running distance upon endurance exercise of *endospanin-2<sup>-/-</sup>* mice compared to their WT littermates (n=5 per genotype) (J) Wheel voluntary activity of *endospanin-2<sup>-/-</sup>* mice compared to *WT* mice (n = 5 per genotype). Results are expressed as means ± sem and were analysed by unpaired t-test except for panel H which was analysed by one-way ANOVA; \* p < 0.05, \*\* p<0.01, \*\*\* p < 0.001

**Supplemental Table 1:** List of specific primers used for qPCR gene expression analysis

	sense	antisense
m endospanin-1	GGGCTGACTTTTCTTATGCTG	CCCAGTGGTGAAGAAATACGC
m endospanin-2	GCCCTTCCGATATAACAACCA	CTCCTTACACGCGTTGC
h endospanin-1	GGCCTTATTCGTCCTGA	TATCCGTCGGACGTGGACT
h endospanin-2	CAAATACTGCCCCCTTTGTTCTATT	TATCCGTCGGACGTGGACT
Mhc2a	CGA GGC TGA CTC GTC CTG CT	GGG GCA GCC TCC CCG AAA AC
Mhc2b	CCA GGC TGC GGA GGC AAT CA	TGC TCG GCC ACT CTC CTG CT
Mhc2x	AAGCTTCAAGTTTGGACCCACGGT	TCGGCGTCGGAACATCATGGC
Igf1	AGCGGGCTGCTTTTGTAGG	TTACTTCAACAAGCCCACAGG
Mgf1	CCA AGA CTC AGA AGT CCC CGT CC	TCC TTC TCC TTT GCA GCT TCG TTT
Mgf2	CCA AGA CTC AGA AGT CCC CGT CC	GTA GGT CTT GTT TCC TGC ACT TCC
Nd1	GTTGGTCCATACGGCATT	TGGGTGTGGTATTGGTAGGG
Cox1	ACTATACTACTAACAGACCG	GGTTCTTTTTTCCGGAGTA
Cox2	AACCATAGGGCACCAATGATAC	GGATGGCATCAGTTTTAAGTCC
Ucp3	GGC CCA ACA TCA CAA GAA AT	GCG TTC ATG TAT CGG GTC TT

## Extended experimental procedures

### Mice

For *endospanin-2* knock out mice generation, the targeting construct containing a L1L2\_Bact\_P cassette composed of an FRT site followed by lacZ sequence and a neomycin cassette under the control of the human beta-actin was inserted into the second intron of *leprot11* gene which interrupts the corresponding open reading frame (**Figure S5A**). Chimeric mice were obtained by blastocyst injection (SEAT, CNRS) and germline transmission was confirmed. Mice were backcrossed with C57BL/6J for ten generations and heterozygotes were inbred. *Endospanin-2* knock out allele in mice was verified by qPCR analysis of skeletal muscle mRNA and protein level (**Figure S5B**).

Endospanin-2 over-expression: Endospanin-2 human coding sequence was introduced in an AAV1 vector (Penn Vector Core, University of Pennsylvania) and  $1 \times 10^{11}$  infectious particles were injected intra-muscularly in the gastrocnemius muscle, whereas the contra-lateral limb muscle was injected with control AAV. Endospanin-2 skeletal muscle-specific overexpression was verified by qPCR (AAV-CTL Ct: 36.6 +/- 0.71; AAV Endospanin-2 Ct 17.8 +/- 0.74) and western blot analysis (**Figure S5C**)

### Mitochondrial ROS production in C2C12

Total intracellular  $H_2O_2$  level was detected using 2',7'-dichlorodihydrofluorescein diacetate (H2DCF-DA), a cell permeable non-fluorescent probe which is intracellularly de-esterified and turns into a highly fluorescent 2'-7'-dichlorofluorescein (DCF) once oxidized. Briefly,  $2 \cdot 10^4$  cells were seeded in 96-well plates and incubated with 10  $\mu$ M of H2DCF-DA (Molecular Probes, Life technology) in PBS for 30 min at 37 °C and 5%  $CO_2$ . The fluorescence ( $\lambda_{ex}=488nm$ ,  $\lambda_{em}=530nm$ ) was evaluated using a Tecan Infinite F500 apparatus.

To specifically detect mitochondrial superoxide production, cells were labelled with 2.5  $\mu$ M MitoSOX™ Red (Molecular Probes, Life technologies) for 15 min at 37 °C then incubated with or without antimycin A (50  $\mu$ M) for 30 min. Cells were then centrifuged and washed twice

with PBS. MitoSOX red fluorescence ( $\lambda_{\text{ex}}=510\text{nm}$ ,  $\lambda_{\text{em}}=580\text{nm}$ ) was measured by flow cytometry (FACSCalibur, BD Biosciences).

### **Mitochondria content**

#### *Mitochondrial DNA quantification*

Total genomic DNA from skeletal muscle was isolated by phenol/chloroform extraction after digestion with Proteinase K (100  $\mu\text{g/ml}$ ). Mitochondrial DNA (mtDNA) was quantified by evaluating the relative amounts of nuclear DNA and mtDNA by quantitative real-time PCR. *Nd1* and *Ppia* genes were selected to amplify mt DNA and nuclear DNA, respectively.

#### *Mitrotracker Green staining*

Endospanin-2 over-expressing C2C12 and their respective control cells were trypsinized and incubated at 37°C for 20 min with 100 nM MitoTracker Green FM dye (Molecular Probes, Life Technologies), a mitochondrial-specific fluorescent probe commonly used to evaluate mitochondrial mass. Samples were washed three times in Phosphate-Buffered Saline (PBS) and analyzed by flow cytometry on a FACSCalibur apparatus (Becton Dickinson, San Jose, CA).

### **Mitochondria isolation from skeletal muscle**

Mice were euthanized by cervical dislocation, and their quadriceps and gastrocnemius muscles were immediately placed in cold PBS. Fat and connective tissues were removed. Then muscles were cut into small pieces and incubated in trypsin-EDTA solution for 15 min at 4°C. Samples were rinsed with mitochondrial isolation buffer (300 mM sucrose, 5 mM TES, 0.2 mM EGTA, pH 7.2) and homogenized with a glass tissue grinder. Homogenates were centrifuged at 800 *g* for 7 min, supernatants were collected and spun twice at 8,800 *g*. Final pellets were resuspended into cold mitochondrial respiration medium (Mir05). For Erk and Stat3 mitochondrial localization, mitochondria were isolated using superparamagnetic microbeads conjugated to anti-TOM22 antibody (# 130-096-946 Myltenyi Biotec) following manufacturer's instructions, which enables to get highly pure mitochondrial fraction. Fraction purity and ER contamination were checked by western blot analysis using OXPHOS antibody cocktail (MitoSciences, Abcam) and calnexin (Stressgen) antibodies (**Figure S4A**).

### **TBARS Assay**

MDA levels from skeletal muscle tissue were quantified using TBARS kit (Cayman Chemical) following manufacturer's instructions. Briefly, 25 mg of muscle was homogenized in 250  $\mu$ l of RIPA buffer containing protease inhibitors. Homogenate was centrifuged at 1,600  $g$  for 10 min at 4°C and the supernatant fraction was used for analysis. MDA-TBA adducts are formed in acidic condition at high temperature (90-100 °C) and detected colorimetrically at 530 nm (Tecan Infinite F500 apparatus, Tecan Systems).

### **Catalase activity**

Muscles were lysed in phosphate buffer using a polytron homogenizer. Samples were centrifuged at 15,000  $g$  at 4 °C for 15 min. Experiment started by adding 2  $\mu$ L of the resulting supernatant into 198  $\mu$ L assay buffer (phosphate buffer containing 14 mM H<sub>2</sub>O<sub>2</sub>). Optical density at 240 nm was monitored every 10 sec for 3 min using Tecan Infinite F500 apparatus (Tecan systems) and compared to a standard curve obtained by diluting different amounts of catalase. Results were expressed as unit of catalase activity per mg of protein.

### **Oxygen consumption on cells and permeabilized skeletal muscle fibers**

C2C12 cells (1 million cells/ml) suspended in cell culture media (DMEM + 10% FBS) were placed into the chambers of the O2K oxygraph (Oroboros Instruments, Innsbruck, Austria), operating at 25°C. Routine respiration (R) was measured 20 min later. Oligomycin (2  $\mu$ g/mL) was injected into the chambers to obtain the leak respiration rate (4o). Then, pulses of FCCP (1  $\mu$ M) were added into the chambers until maximal oxygen consumption was reached (3u). After cervical dislocation, EDL muscles were excised and placed into a Petri dish containing ice-cold biopsy preservation solution (BIOPS) and permeabilized fibers were prepared as previously described fibers (45) (3 to 6 mg wet weight) were placed into the O2K oxygraph chambers. Glutamate (10 mM) and malate (2 mM) were added to obtain state 2 respiration. To measure ADP-coupled oxygen consumption also-called state 3, 2.5 mM ADP was injected into the chambers. A further addition of succinate (10 mM) was performed to estimate the entire OXPHOS capacity. Finally, complex II-linked respiration was evaluated after complex I inhibition with rotenone (1  $\mu$ M). Experiments were performed at 25°C.

### **Quantitative RT-qPCR**

Total RNA was extracted from snap-frozen tissues or cells by using guanidinium thiocyanate/phenol/chloroform and Trizol reagent (Invitrogen, Life Technologies) respectively. cDNA were synthesized using commercially available reagents (Superscript II kit; Applied Biosystems). Gene expression levels were measured by quantitative real-time PCR reactions (RT-qPCR) using the Brilliant III SYBR Green QPCR Master Mix (Agilent Technologies) on a Mx3005 apparatus (Agilent Technologies) using specific primers (Supplemental Table 1). Gene expression was normalized to *Ppia* and expressed as indicated in the figures.

### **Protein extraction and western blot analysis**

Skeletal muscle, mitochondrial and cell protein extracts were separated by SDS-PAGE, transferred onto PVDF membranes (Hybond-P GE Healthcare) and immunoblot analyses were carried out using antibodies directed against UCP3 (#PA1-055, ThermoScientific), P-Akt (#9271, Cell Signaling Technology), Akt (#9272, Cell Signaling Technology), P-ERK1/2 (#9101 Cell Signaling Technology); ERK1/2 (#9102 Cell Signaling Technology), P-Stat3 Ser 727 (#9134 Cell Signaling Technology), P-Stat3 Tyr 705 (#9131 Cell Signaling Technology) and Stat3 (#9139 Cell Signaling Technology); GAPDH (#sc 25778 Santa Cruz Biotechnology), Actin (#sc-16-16 Santa Cruz Biotechnology) and Endospalin-2 (LEPROTL1) (#sc-87194 Santa Cruz Biotechnology); VDAC (#ab34726 Abcam, LC3 (#ab51520 Abcam) and Ulk1 (#ab128859 Abcam) ; Atg5 (#NB110-53818 Novus); Beclin (#AP1055 Calbiochem), according to manufacturer's instructions.

### **Electron microscopy analysis of muscle sections**

Ultrastructural muscle morphology was analysed using transmission electron microscopy as previously described (45).

### **Immunofluorescence microscopy.**

Indirect immunofluorescence localization was performed on **C2C12** cells grown on glass coverslips. Cells were fixed with 3% paraformaldehyde in PBS and permeabilized by 0.01% Triton X-100 in PBS for 2 min at room temperature. Both primary (Rabbit polyclonal

antibodies to endospalin-1 or endospalin-2 previously described (11)), anti-LC3 mouse mAb (#ab51520 Abcam), LAMP-1 (#553792 BD Biosciences) and secondary antibody (Alexa488-conjugated donkey anti-rabbit IgG, Cyanin 5-conjugated donkey anti-mouse IgG both from Jackson ImmunoResearch and Alexa555-conjugated goat anti-rat IgG from Invitrogen) incubations were carried out in PBS containing 5% horse serum for 30 min at room temperature. The coverslips were mounted on slides by using Mowiol 4-88-containing mounting medium (Calbiochem). Confocal microscopy was performed with an LSM 780 confocal laser-scanning microscope (Zeiss) using a 63x/1.4 numerical aperture oil immersion lens. Triple-label immunofluorescence signals were sequentially collected using single-fluorescence excitation and acquisition settings to avoid crossover. Images were assembled using Adobe Photoshop software.

### ***In situ* isometric contractile properties of the EDL muscle**

The mice were anesthetized with intraperitoneal injections of sodium pentobarbital (60 mg/kg), prolonged if necessary by supplementary doses (30 mg/kg).

Briefly, all the muscles of the right hindlimb were denervated, except the extensor digitorum longus (EDL) muscle. Then, the limb was fixed in isometric conditions and was immersed in a bath of paraffin oil thermostatically controlled (37°C). The limb was stabilized by using a combination of bars and pins, and the EDL muscle was maintained in horizontal position. Afterward, the EDL muscle was isolated from surrounding tissues, and its distal tendon was connected to a force transducer (Grass FT 10; Grass Instruments, West Warwick, RI, USA). The muscle length was adjusted to produce a maximal isometric tension. Stimulating and reference electrodes (Teflon-coated platinum) were maintained by micromanipulators. Contractions were induced by stimulation of the EDL nerve (0.2/ms pulses) through monopolar platinum electrodes at twice the minimum voltage required to obtain the maximal twitch response. The reference electrode was inserted into adjacent denervated muscle mass. The following parameters were recorded: a single maximal twitch, from which the maximal twitch tension, the time to peak, and the half-relaxation time were measured; and the tension/frequency relationship (for stimulation frequencies ranging from 16 to 100 Hz),

which allowed the determination of maximum tetanic tension  $P_0$  obtained for a 100-Hz stimulation frequency and of fatigue index  $P_{40}/P_0$  (ratio of the tetanic tension at 40 Hz to  $P_0$ ) (47).

### **Myosin heavy chain analysis**

Muscle contractile phenotype was determined through analysis of MHC composition. Slow (MHC I) and fast (MHC IIa, IIx, and IIb) MHC isoforms were separated by one-dimensional SDS-PAGE, as previously described (44). Myofibrillar proteins were extracted from 10 mg of muscle powder in a buffer containing 20 mM Tris, pH 7.4, 4 mM EGTA, 10 mM EDTA, 0.1% pepstatin, and 1% PMSF. Protein estimation was determined by a Lowry assay to prepare the samples with a final quantity of 4  $\mu$ g. Protein separation was performed on 7.5% acrylamide-bisacrylamide (99:1) SDS-PAGE at 14°C and for 22 h (180 V, 13 mA). Then, gels were sensitized with glutaraldehyde and silver stained. GS-800 Imaging densitometer and QuantityOne Software (Bio-Rad, Hercules, CA, USA) were used to determine the relative proportions of the different MHC isoforms in each muscle.

### **Myosin heavy chain immunofluorescence**

Upon automated binning and measuring color intensity in individual color channels, unstained fibers were classified as MHC2b, fibers staining green were identified as MHC2a fibers, fibers staining red were identified as MHC2x. Fibers staining in green and red have been identified as hybrid fibers, provided staining intensity in both fibers exceeded a previously set threshold of 40 arbitrary units. The percentage of fibers designated MHC2a, MHC2x, MHC2b or hybrid were computed relative to the total number of fibers counted.

### **PAS Staining**

Muscle glycogen content was measured biochemically and histochemically. After precipitation of glycogen, the pellet was hydrolyzed and glycogen-derived glycosyl units were quantified spectro-photometrically using a glucose kit (hexokinase method; Roche). Conventional staining of glycogen using Periodic Acid Schiff (PAS) was performed on individual muscle sections. The PAS derived signal was converted to 8 bits grayscale and



optical density per pixel was examined. Mean optical density of the sections was examined and used as a semi-quantitative measure of muscle glycogen content.

### **IPGTT**

For tolerance tests, 1 g/kg of mice body weight of glucose was injected intraperitoneally and blood glucose was measured as indicated.

### **Muscle insulin sensitivity analysis**

Mice were injected intraperitoneally with 0.75 mU of insulin per g of body weight. 8 minutes later, mice were euthanatized and quadriceps muscles were harvested carefully for subsequent pAkt analysis.

### **Supplemental reference**

47. Picquet F, Falempin M. Compared effects of hindlimb unloading versus terrestrial deafferentation on muscular properties of the rat soleus. *Exp Neurol*. 2003;182(1):186–194.